



Traces, Profiles, and Extraction Tables for the COS FUV Channel at Lifetime Position 4

Marc Rafelski¹, William J. Fischer¹, Nick Indriolo¹, and Julia Roman-Duval¹

¹ Space Telescope Science Institute, Baltimore, MD

14 February 2019

ABSTRACT

We report on the creation of the COS FUV trace and profile reference files at the fourth lifetime position (LP4). We also describe the creation of spectral extraction tables for the TWOZONE and BOXCAR algorithms. These reference files include calibration products for all the apertures, spectral elements, and central wavelength settings, except for G130M/1055 and G130M/1096, which remain at LP2. The reference files were created using the same vetted methods as at LP3. The traces and profiles at LP4 are quite similar to those at LP3, and the minor variations are likely due to different characteristics of the detector at the new location and due to the optics resulting in a different optical path (field angle) and focus at LP4.

Contents

1. Introduction	2
2. Observations	3
3. Reference File Creation	3
3.1 Overview of Iterative Process for Traces and Profiles	4
3.2 1-D Spectral Extraction Table	4
3.3 Creation of Traces	5
3.4 Creation of Profiles	6

3.5 TWOZONE Spectral Extraction Table	8
4. Science Validation	9
Acknowledgements	11
Change History for COS ISR 2018-21	11
References	11
Appendix A	12
Appendix B	13

1. Introduction

The Cosmic Origins Spectrograph (COS) far-ultraviolet (FUV) channel consists of two stacks of micro-channel plate (MCP) detectors to convert incoming photons to clouds of electrons, and cross-delay line (XDL) anodes to determine the time and location of the incident photons. These electron clouds are characterized by a pulse height amplitude (PHA), which describes the number of electrons in the cloud. The response of the MCPs decreases with electron extraction, resulting in reduced PHAs as the detector is used (Sahnou et al. 2011). This phenomenon is referred to as gain sag. When the PHA declines below 3, it becomes difficult to separate out photon events from the background, and the flux loss exceeds 5%. The flux loss increases steeply with decreasing gain below 3, which leads to the resultant spectrum having “holes” where the data cannot be reliably extracted due to gain sag. These holes compromise the quality of the COS/FUV spectra.

To mitigate the effect of gain sag and provide the community with access to unsagged regions of the FUV detector, the location of the COS FUV spectrum is periodically moved to a new location on the detector (called a lifetime position or LP). The fourth lifetime position (LP4) is located $-5.0''$ below LP1 ($-2.5''$ below LP3), and the move occurred on October 2, 2017. This is illustrated in Figure A.1 of the COS Data Handbook (Rafelski et al. 2018), which shows the relative positions of the different lifetime locations and the modal gain (see also Roman-Duval et al. 2018).

LP3 and LP4 are sufficiently close to gain-sag holes from previous lifetime positions that a “TWOZONE” extraction algorithm is required rather than the original “BOXCAR” algorithm (Proffit et al. 2015; see also Roman-Duval et al. 2016 and Roman-Duval et al. 2018). The BOXCAR algorithm rejects a wavelength bin if any sagged or bad pixels are included within the extraction region, even if at the edge of the extraction box, which would have little impact on the extracted spectrum. To avoid discarding columns with sagged or bad pixels at the edges, the TWOZONE algorithm only excludes wavelength bins with sagged pixels sufficiently close to the target spectrum by using a variable height extraction box based on the enclosed energy contours, which depends on the cross-dispersion profile at each wavelength.

The TWOZONE extraction requires three reference files to be updated for LP4: the TWOZXTAB, TRACETAB, and PROFTAB. The TWOZONE spectral extraction table (TWOZXTAB) provides the parameters for the TWOZONE algorithm, including

the area of the detector to search for the source spectrum and the size and location of the background regions. It is similar to the 1-D spectral extraction table (XTRACTAB) reference file which provides parameters for the BOXCAR algorithm, and we describe the update to this reference file for LP4 here as well. The TRACETAB stores the trace correction to straighten the spectral images for each central wavelength (cenwave). Lastly, the PROFTAB contains the 2-D cross-dispersion profile shape for each cenwave, needed to calculate the enclosed energy contours. The reference file format and the algorithms that use the files are described in more detail in Proffit et al. (2015).

In this report we describe the creation of the above-mentioned reference files for LP4; the data are described in Section 2. The creation of the reference files is an iterative process which depends on the flats as described in Fischer et al. (2018) and is outlined in Section 3.1. The update to the spectral extraction tables is described in Sections 3.2 and 3.5. In Sections 3.3 and 3.4 we describe the creation of the traces and profiles. In Section 4 we discuss the science validation of the new reference files. Lastly, in Appendix A we provide information on the software used to create the reference files, and in Appendix B we provide additional figures corresponding to different central wavelengths or optical elements.

2. Observations

The spectra used to derive the traces, profiles and spectral extraction parameters were obtained in April 2017 via program 14910, “Fourth COS FUV Lifetime Position: Cross-Dispersion Profiles, Flux, and Flat-Field Calibration” (PI M. Rafelski). Data were obtained at all cenwaves except for the blue modes (G130M/1055 and G130M/1096) at signal-to-noise (S/N) $\sim 50 \text{ resel}^{-1}$. The hot subdwarf WD 0308–565 is the primary target due to its being a flux standard and a time-dependent sensitivity (TDS) monitoring target. Its spectrum has a relatively flat shape without absorption and emission lines, enabling characterization of the cross-dispersion profiles. However, because the spectral energy distribution (SED) is very blue, there is insufficient flux at the red wavelengths (G160M grating) to meet our S/N goals. Therefore, the white dwarf GD 71 was also observed to more efficiently calibrate the longer wavelength Segment A in the G160M modes. All cenwaves were observed at all four FP-POS, as this program executed before the COS2025 policy was in effect (Oliveira et al. 2018). These spectra are tabulated in Table 1 of Fischer et al. (2018).

3. Reference File Creation

This section describes the creation of the XTRACTAB and TWOZXTAB spectral extraction tables, the TRACETAB spectral traces, and the PROFTAB 2-D spectral profiles.

3.1 Overview of Iterative Process for Traces and Profiles

The creation of the traces and profiles depends iteratively on both the flats and the spectral extraction tables (XTRACTAB and TWOZXTAB). Therefore, the creation of the profiles went through a multi-step process as described here. For the first steps, until the LP4 flat field is created, CalcOS is run with a grid wire shadows only flat. This flat corrects for the grid wire shadows, which do not vary with LP and are the largest source of fixed-pattern noise in the detector (Ely et al. 2011; Debes et al. 2016).

First, the data are processed in order to create the XTRACTAB file at LP4. The first pass is run with the default LP4 extraction table calculated by applying an offset to the LP3 XTRACTAB file based on the distance moved on the detector from LP3 to LP4. This results in an extraction used to determine the extraction parameters for the XTRACTAB file as described in Section 3.2. This also produces the *corrtag* files to create the initial traces and profiles, as described in Sections 3.3 and 3.4. Using this initial profile, the TWOZXTAB is created as described in Section 3.5. At this point the initial set of reference files is used to process the data to enable creation of the flats as described in Fischer et al. (2018). With the new flats in hand, the above process is repeated. Specifically, the data are processed with the LP4 flats and XTRACTAB in BOXCAR mode, and the output is used to create final profiles and flats. This final profile is used to create the final TWOZXTAB.

3.2 1-D Spectral Extraction Table

The XTRACTAB is the 1-D spectral extraction table used with the BOXCAR extraction algorithm. It provides the information needed to extract the spectrum from geometrically corrected images for each optical element and cenwave. Since the trace of the spectrum has a slope, it provides the slope, intercept, and height of the target spectral extraction box. It also provides the location and height of the background extraction boxes. Even though the recommended extraction algorithm at LP4 is TWOZONE, the XTRACTAB is still needed for the WAVECORR calibration and to define the encircled energy (EE) of the profiles. The format of this file is provided in Table 3.9 of Rafelski et al. (2018).

To create the XTRACTAB at LP4, the initial position of the traces is obtained from the LP3 XTRACTAB and the y-shift from LP3 to LP4 (lower by ~ 28 pixels), which is then used to measure the slope and y-intercept from the target and lamp spectra in flat-fielded and thermally and geometrically corrected spectral images. The background locations have to be adjusted manually, as we do not want the background calculated too close to the Primary Science Aperture (PSA), on top of the Wavelength Calibration Aperture (WCA), or in a sagged region of the detector from previous LPs. The smoothing box to smooth the background region is left at the LP3 value (100 pixels). Figure 1 shows an example of the PSA, WCA, background regions, and locations of the different lifetime positions shown on top of the 2-D spectral image and collapsed 1-D data for the delivered XTRACTAB.

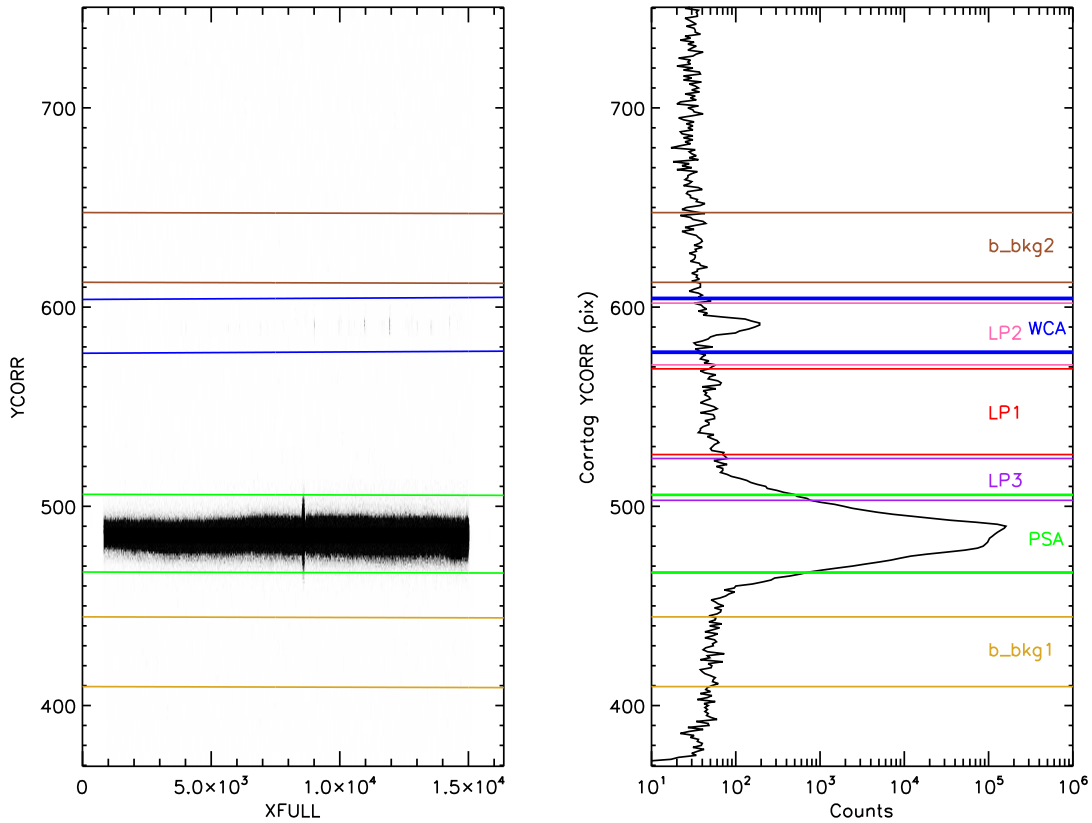


Figure 1. *Left:* A 2-D spectral image of G130M/1291 FUVB FP-POS=1. *Right:* The collapsed 1-D data with the regions from the XTRACTAB and different lifetime positions labeled. The green and blue lines show the LP4 PSA and WCA areas. The yellow and brown lines show the two background regions. The red, pink, and purple lines show the areas of LP1, LP2, and LP3. Note the overlap of the PSA and LP3, which is why the TWOZONE spectral extraction is recommended. The background locations are chosen not to overlap with any of the other regions while being as close as possible to the PSA. While the LP4 WCA overlaps with the LP2 PSA, it is not a concern; see White et al. (2019).

3.3 Creation of Traces

The COS FUV trace maps the centroid of the spectrum in Y (cross-dispersion direction) as a function of the column number (XCORR; dispersion direction) and is defined by the residual geometric distortion effects. It varies between cenwaves and LPs because they occupy different footprints on the detector. Since the TWOZONE algorithm uses a smaller variable height extraction region than BOXCAR, it therefore requires the use of TRCECORR and ALGNCORR to remove the residual geometric distortion in Y (straightening of the trace) and shift the spectrum in the cross-dispersion direction (shifting the y placement) to align it with the template profile for a given grating and

cenwave. To do this, the trace of the spectral image for each setting has to be determined and provided to CalcOS via the TRACETAB reference file. The TRACETAB is a table that provides the variation of the centroid of the spectrum as a function of XCORR, and it is created based on the *corrtag* files as described in Section 3.1. The format of the TRACETAB is provided in Table 3.17 of Rafelski et al. (2018).

The trace is measured in the following way. First the data are filtered for prominent airglow lines Ly α (wavelengths from 1212 to 1219 Å are masked) and O I (wavelengths from 1300 to 1310 Å are masked) and for the wavecal lamps. The routine builds a 2-D image in XCORR and YCORR using CalcOS `bin_corrtag` and then calculates the flux-weighted Y centroid for each column (XCORR) and interpolates over any bad data values. It then computes the composite trace by aligning the available data by the mean of the trace (both for different FP-POS and for different targets if applicable) and taking the flux-weighted average of all the traces for the given grating and cenwave.

If a region of data has very poor S/N, such as the bluest wavelengths of 1222, then it splices in the trace from cenwave 1291 over that region. These regions to be spliced are manually selected. The trace is spliced in by fitting a line to the difference between the two traces, adjusting the 1291 trace by the slope of that line, and then replacing the relevant wavelength range. This is a reasonable approach because the footprint on the detector of 1291 is closest to that of 1222. Since the trace is fixed in detector space (no effects from optics or wavelength), one would expect the 1222 and 1291 traces to be very similar. This is primarily to have a reasonable trace over the entire detector region, even though the sensitivity in these wavelength regions is low enough that any data are unlikely to be scientifically useful.

The top panel of Figure 2 shows an example of a trace for G130M/1291 FUVB, where the solid black line shows the new LP4 trace and the dotted blue line is the trace from LP3. The bottom panel of Figure 2 shows the difference between the trace at LP3 and LP4. The two traces are very similar, with differences likely due to different residual geometric distortion and other small-scale structure variations between LP4 and LP3.

3.4 Creation of Profiles

The PROFTAB reference file provides the 2-D profile of a point source as a function of column number (XFULL), as they are determined by the optics and are thus fixed in XFULL for a given cenwave. The profile is generated from the combined spectra used to create the trace, with the trace described in Section 3.3. Therefore the small-scale detector structure observed in the trace is already removed, the profile is flat in the dispersion direction, and the flux-weighted centroid of the profiles is the same in all the columns. The profiles are measured for the PSA, and then are copied over for the Bright Object Aperture (BOA). The profiles are only tabulated over a portion of the full height of the FUV detector, and *ROW_0* specifies to which row in the full-sized array the first row in the profile corresponds. The format of the PROFTAB is provided in Table 3.18 of Rafelski et al. (2018).

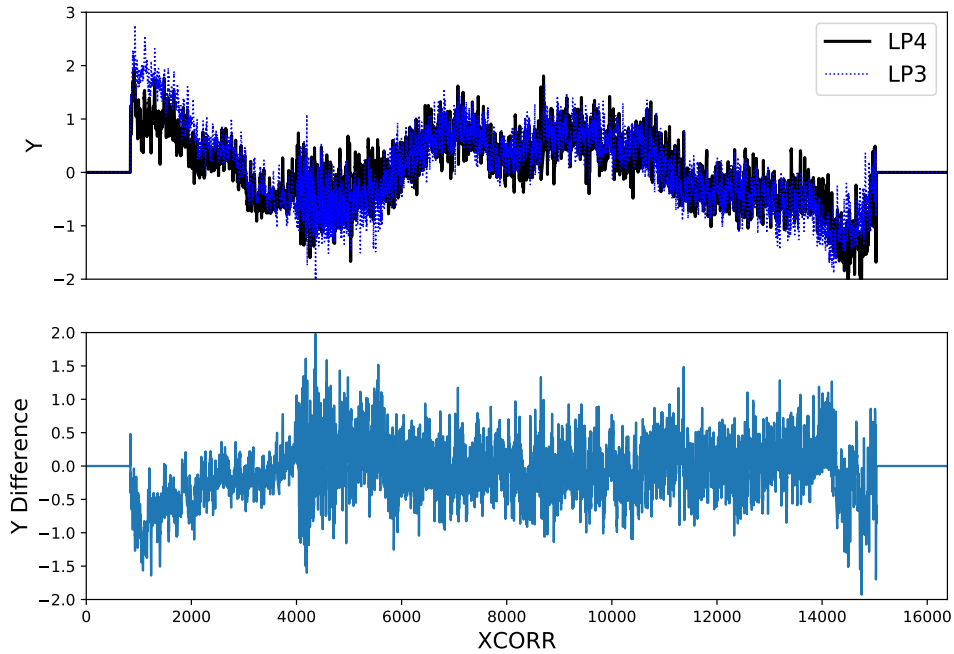


Figure 2. *Top:* The trace of G130/1291 FUVB for LP4 in solid black and LP3 in dotted blue. The pixel-to-pixel variations observed in the trace on scales of hundreds of pixels are due to residual geometric distortion and small-scale structure. *Bottom:* The difference between the trace at LP3 and LP4. The trace at LP4 is similar to LP3, with some minor differences due to its location on the detector below LP3, and therefore it shows slightly different geometric distortions and structure.

The profile is measured in the following way. The routine starts with the aligned and airglow-filtered data from the TRACETAB creation described above. This means the input to the profile generation has already been corrected for the shape of the trace. It takes these data products from generating the trace and bins the events into a 2-D image in XFULL and YFULL, truncates it in the cross-dispersion direction based on the XTRACTAB extraction box, and pads it such that anything outside the extraction area defined in the XTRACTAB is 0. It then linearly interpolates over the airglow lines and the left and right sides of the profiles. Finally, the profiles are normalized such that each individual column sums to unity.

Figure 3 shows an example of a profile for G130M/1291 FUVB, where the top panel is the new LP4 profile, the middle panel is the LP3 profile, and the bottom panel is the percent difference of the two profiles. The difference in the interpolated region near XFULL \sim 9000 is due to an increase in the interpolated area for the Ly α airglow line at LP4. The two profiles are very similar, with differences likely being caused by

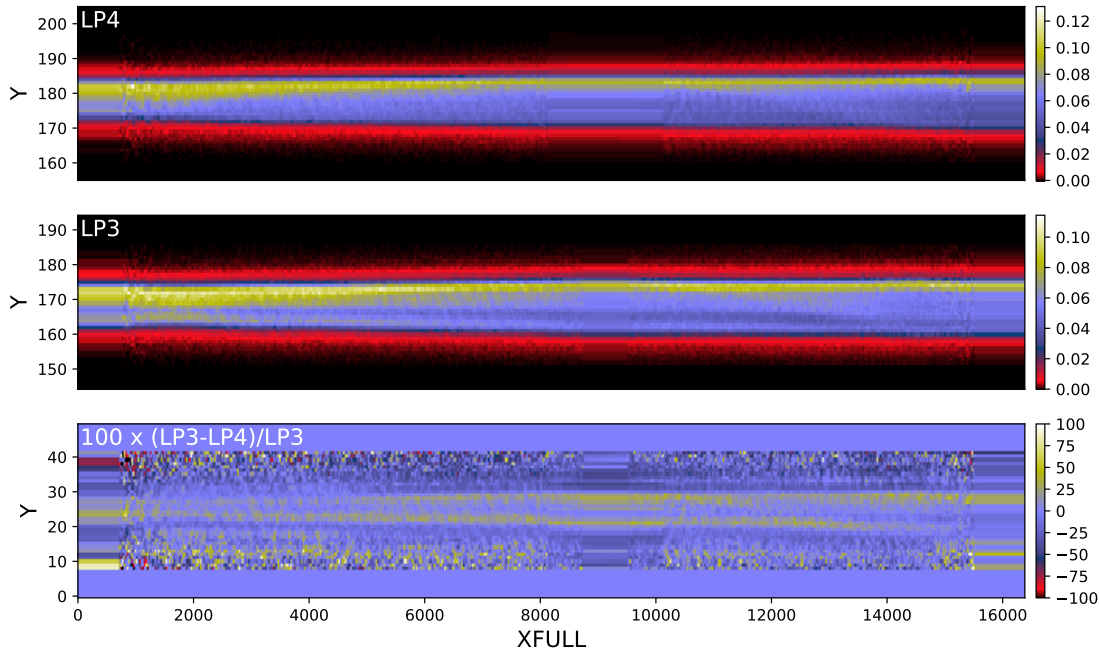


Figure 3. *Top:* The profile of G130/1291 FUVB at LP4. *Middle:* The profile of G130/1291 FUVB at LP3 for comparison with LP4. *Bottom:* The percent difference between the LP3 and LP4 profiles. The profiles at LP3 and LP4 are quite similar, and the differences between the two profiles reflect the slightly different optical path (field angle) and focus, which both affect the shape and width of the profiles.

the slightly different optical path (field angle) and focus, which both affect the shape and width of the profiles.

3.5 TWOZONE Spectral Extraction Table

The TWOZXTAB is the spectral extraction table used with the TWOZONE extraction method. It provides the starting values to search for the center of the target spectrum and the locations of the background regions. There are several differences between this table and the XTRACTAB. First, the TWOZXTAB sets the center of the spectrum to the profile center from the PROFTAB and does not provide a slope. The slope of the trace is already removed in the TRCECORR step based on the TRACETAB. Second, unlike the XTRACTAB, the TWOZXTAB does not define the extraction box since the 2-D spectra are extracted based on the EE calculated by CALCOS from the template profiles (Proffitt et al. 2015). We note that the TWOZXTAB only provides the center of the profile, the background regions, and the fraction of flux below the different boundaries to calculate the EE. The *b_spec* and *height* values in the TWOZXTAB only define the search range to find and align the target spectrum with the template profile. The format of the TWOZXTAB is provided in Table 3.19 of Rafelski et al. (2018).

4. Science Validation

Even though the profiles and traces are generated with the same vetted methodology as those at LP3, we validate them by using the new reference files to calibrate data with CalCOS and ensure that the results are consistent with expectations from other data or models. First, we compare 1-D spectra extracted using the BOXCAR algorithm to spectra extracted using the TWOZONE algorithm with the new profiles and traces. For this test we use the same dataset as for the creation of the profiles and traces (PID 14910), and extract the spectra using CalCOS with default parameters for each extraction type. This includes the new spectral extraction tables as described in Sections 3.2 and 3.5 and the new flats described in Fischer et al. (2018). Since by construction the TWOZONE algorithm in CalCOS extracts spectra inside the 99% EE contour (100% being set by the box in the XTRACTAB), one expects $< 1\%$ difference between net counts in the spectra extracted with BOXCAR and TWOZONE.

Figure 4 shows an example from this testing for G130M/1291 FUVB FP-POS=2, and all the different settings show similar results. The top panel plots the net count rate for the two algorithms, and they are mostly identical and therefore overlap significantly. The difference between these two curves is plotted in the bottom panel, showing very small residuals except at wavelengths with strong emission lines (in this case, at Ly α at 1216 Å). This difference is due to the fact that the airglow fills the aperture, and therefore it does not follow the profile, which is the response to a point source. Hence, one expects many more airglow counts in the BOXCAR compared to the narrow TWOZONE extraction optimized for a point source. The middle panel compares the data quality (DQ) values via the parameter n , where $DQ = 2^n$. The DQ values flag suspect pixels, and the only difference we expect is for pixels flagged as low-response regions ($DQ = 2^{10}$), as those would be ignored by the TWOZONE algorithm along the edges. Indeed, the figure shows that the DQs are basically the same except at wavelengths where the edges of the BOXCAR extraction window are gain-sagged from LP3 observations.

Second, we compare the enclosed energy (EE) contours computed by CalCOS using the profiles and output in the *x1d* files to those manually computed from a different dataset from the data used to produce the profiles. We use data from the LP4 resolution program PID 15366 (PI A. Fox), as the exposures also have high S/N (see Fox et al. 2018). However, these data cannot be used for the generation of the profiles because the target AzV 75 shows stellar absorption lines, providing holes in the wavelength space where the EE cannot be accurately calculated.

Figure 5 shows a 2-D spectrum for G130M/1222 FUVB FP-POS=1 from PID 15366, and the other settings show similar results. The EE computed by CalCOS from the profiles (output in the calibrated and extracted *x1d* files) is shown in red and cyan for 99% and 80% EE, respectively, while the direct measurements on the resolution program data are shown in green and blue. The green and red contours and blue and cyan contours are very similar except at the locations of the stellar absorption lines

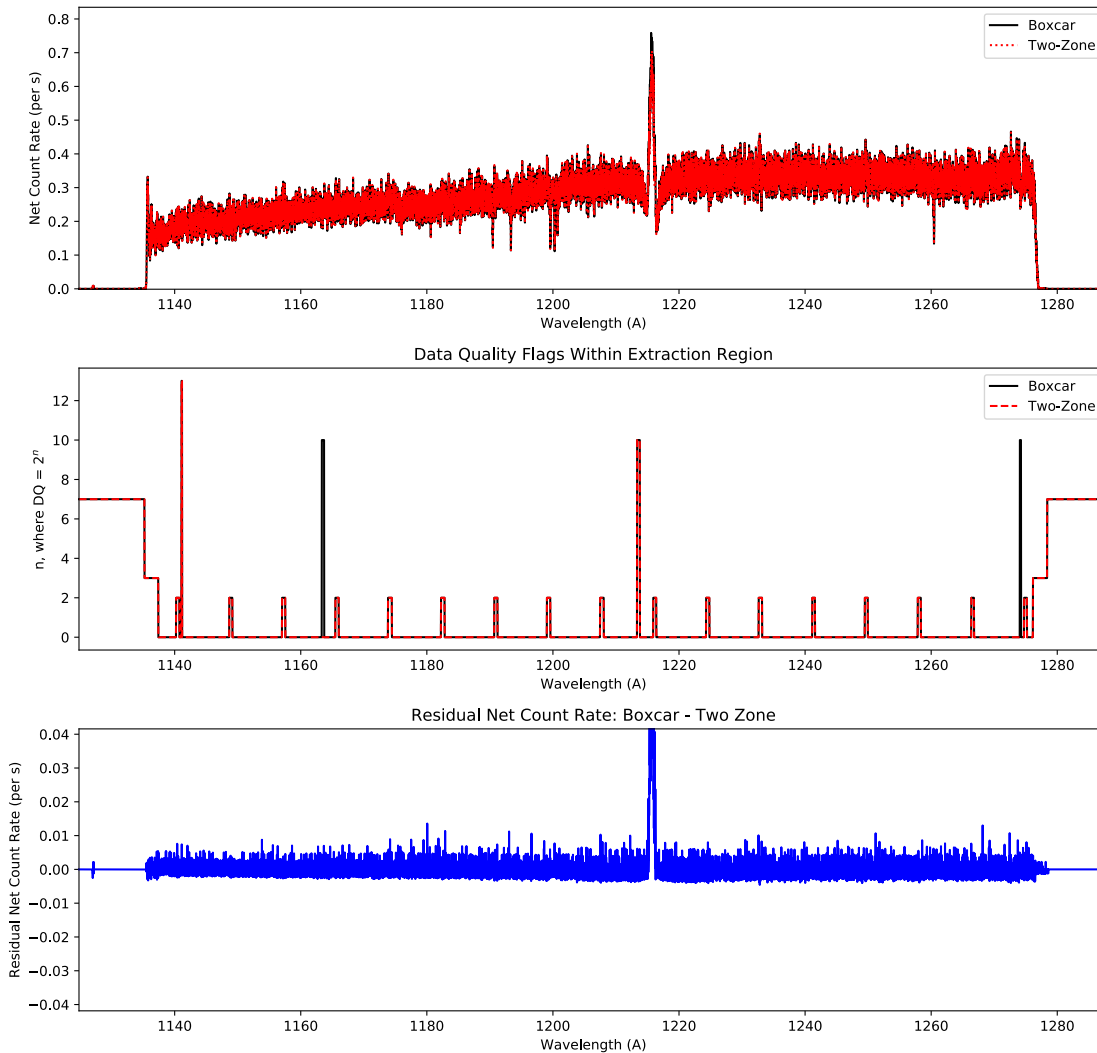


Figure 4. Comparison of a spectrum of WD 0308–565 from PID 14910 extracted via the BOXCAR and TWOZONE algorithm for exposure 1d1e101oyq with settings G130M/1291 FUVB FP-POS=2. This demonstrates the validity of the new profiles and traces for extracting 1-D spectra using the TWOZONE algorithm compared to a standard BOXCAR extraction.

(shown as black bands in the image). At those locations the flux goes to zero, and thus the EE cannot be accurately determined. The slight difference between the 99% contours is because the data are of lower S/N than the profile data, which is obtained from a stack of all four FP-POS. Hence, the noise in the red contour is less than observed in the green contour. The general agreement of the different contours validates the EE calculated from the profiles on different data and shows that they are properly defined.

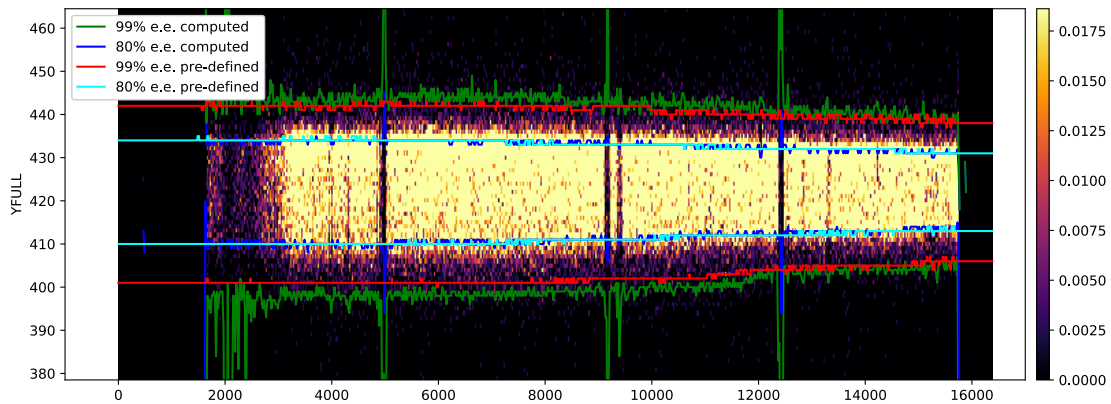


Figure 5. Comparison of enclosed energy (EE) contours as determined from the profiles and directly from a single 2-D spectrum from a different dataset (PID 15366 for exposure ldm701qng with settings G130M/1222 FUV A FP-POS=1). The EE computed by CalCOS from the profiles is shown in red and cyan for 99% and 80% EE, respectively (“pre-defined”), while the direct measurements on the 15366 data are shown in green and blue (“computed”). Note that the black bands are stellar absorption lines, and the EE contours cannot be determined at those locations in the PID 15366 data. This demonstrates the validity of determining the EE from the new profiles compared to measuring it on individual 2-D spectra.

Acknowledgements

We acknowledge the entire COS team for their support in moving to lifetime position 4 and enabling the calibration of the detector.

Change History for COS ISR 2018-21

Version 1: 14 February 2019 – Original Document

References

- Debes, J. H., Becker, G., Roman-Duval, J., et al. 2016, COS ISR 2016-15, “Third COS FUV Lifetime Calibration Program: Flatfield and Flux Calibrations”
- Ely, J., Massa, D., Ake, T., et al. 2011, COS ISR 2011-03, “COS FUV Gridwire Flat Field Template”
- Fischer, W. J., Rafelski, M., & de Rosa, G. 2018, COS ISR 2018-20, “Flat Fields and Flux Calibrations for the COS FUV Channel at Lifetime Position 4”
- Fox, A., James, B., Roman-Duval, J., Rafelski, M., & Sonnentrucker, P. 2018, COS ISR 2018-07, “The Spectral Resolution of the COS FUV Channel at Lifetime Position 4”
- Oliveira, C., de Rosa, G., Mackenty, J., et al. 2018, COS ISR 2018-16, “COS2025: A New Strategy to Prolong the Lifetime of the COS/FUV Detector to 2025”

Profitt, C. R., Bostroem, K. A., Ely, J., et al. 2015, COS ISR 2015-03, “Changes to the COS Extraction Algorithm for Lifetime Position 3”

Rafelski, M., et al. 2018, *Cosmic Origins Spectrograph Data Handbook*, Version 4.0 (Baltimore: STScI)

Roman-Duval, J., Ely, J., Debes, J., et al. 2016, COS ISR 2016-01, “Optimization of Lifetime Position 3 of the COS/FUV Detector”

Roman-Duval, J. Indriolo, N., de Rosa, G., et al. 2018, COS ISR 2018-14, “Exploratory Phase for Optimizing Lifetime Position 4 of the COS/FUV Detector”

Sahnow, D. J., Oliveira, C., Aloisi, A., et al. 2011, Proc. SPIE, 8145, 81450Q (also COS ISR 2011-05, “Gain Sag in the FUV Detector of the Cosmic Origins Spectrograph”)

White, J., Indriolo, N., & Roman-Duval, J. 2019, COS ISR 2018-15, “Performance of the CalCOS FUV WAVECORR Algorithm at Lifetime Position 4”

Appendix A

Appendix A describes the software used to create the reference files, and it may not be of interest to all readers as the software is not publicly available.

The XTRACTAB is created by the program `make_lp4_XTRACTAB.pro`, which is in the directory `ldx_lifetime4`. This program and those described below are in the `cos/ref_files` repository on the internal STScI GitLab repository. To create the XTRACTAB at LP4, `make_lp4_XTRACTAB.pro` is provided the LP3 XTRACTAB and the y-shift from LP3 to LP4 to determine the initial position of the trace, which is lower by ~ 28 pixels on the detector. The resultant parameters are saved out to a file to be manually edited by `print_parameter_file_ldx_lp4.pro`, and then input to `xtractab_table.pro` to create the final XTRACTAB.

The TRACETAB is created by the program `make_traces_profiles.py` in `prof_trace_tab_lifetime4`, which runs on the `corrtag` files as described in Section 3.1. This program creates both the TRACETAB and the PROFTAB by default, or the trace can be generated individually with the function `compile_traces()`.

The PROFTAB is created by the same code that generates the TRACETAB, `make_traces_profiles.py` in `prof_trace_tab_lifetime4`, and it can be run individually with the function `compile_profiles()`. It is intended to be run at the same time as the trace determination, as it depends on the output products from those steps. If run without generating the trace, the function requires the output data products of a previous TRACETAB creation run.

The TWOZXTAB at LP4 is created by the program `2zx_table.pro` which is provided the LP4 XTRACTAB and a parameter file created by `print_parameter_file_2zx_lp4.pro` in `2zxtab_lifetime4`. In turn, the parameter file creation code is provided the PROFTAB and the LP4 XTRACTAB, and it outputs the relevant parameters for the TWOZXTAB including the profile center. Therefore the TRACETAB and PROFTAB are created before the TWOZXTAB.

Appendix B

Appendix B provides additional figures of more segments and cenwaves for Figures 1 through 5. These figures are as described in the relevant figure captions.